

Flat Optical Devices for Grafted Vortex Beams Generation

Hammad Ahmed^{1*}, Xianzhong Chen¹

¹Institute of Photonics and Quantum Sciences, School of Engineering and Physical Sciences, Heriot-Watt University, Edinburgh, EH14 4AS, UK.

*Corresponding author: H.Ahmed@hw.ac.uk

Abstract: Optical vortex (OV) beams possess helical wavefronts that originate from their spiral phase profiles and are typically characterized by a single topological charge. Drawing inspiration from plant grafting, where a scion is joined with a different rootstock, grafted vortex beams (GVBs) are created by combining two or more helical phase distributions of OVs. Traditional experimental approaches for generating GVBs are often complex, bulky, and expensive. In this poster, we present our recent work on generating and controlling GVBs using flat optical metasurfaces. This method enables the development of compact, ultrathin photonic platforms capable of executing sophisticated optical functions that are difficult to achieve with conventional optics. We believe this work will pave the way for new applications in quantum science, optical communication, and particle manipulation.

In conventional OVs, the orbital angular momentum (OAM) distribution on the doughnut-shaped intensity ring is uniform, limiting their use in applications requiring versatile OAM distributions, such as multiparticle trapping. Noncanonical optical vortices with non-uniform OAM distributions have been proposed, but local modulation of OAM remains challenging. GVBs, created by combining two or more spiral phase profiles, offer controllable OAM distribution with constant intensity. Recently, GVBs have attracted attention for their unique properties and potential in particle manipulation. However, generating and manipulating GVBs is complex, requiring additional optical elements, leading to large setups and high costs.

We experimentally demonstrate a metasurface-based method for generating and controlling GVBs that does not rely on traditional optical setups [1]. In this approach, orbital angular momentum and asymmetric singularity distributions are precisely tailored by incorporating specific phase differences into the metasurface design (as shown in Figure 1). Furthermore, we expand this concept to multispectral grafted perfect vector vortex beams (GPVVBs) [2], a novel class of vector vortex beams featuring inhomogeneous polarization and spiral phase structures. This strategy addresses the conventional limitation on the number of topological charges in vortex beams. GPVVBs are produced by superimposing multiple hybrid GPVBs using a multifunctional metasurface, enabling spatially varying polarization profiles and enhanced design versatility [3]. The generated beams can also be dynamically adjusted through a rotating half-wave plate, transforming the metasurface into a tunable optical device.

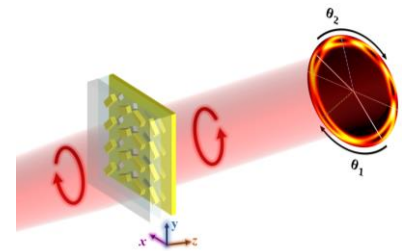


Figure 1: Schematic of GVB generating metasurface.

References

- [1]. Ahmed, Hammad, et al. "Multichannel superposition of grafted perfect vortex beams." *Advanced Materials* 34.30 (2022): 2203044.
- [2]. Wang, Guanchao, et al. "Creating Multispectral Grafted Perfect Vector Vortex Beams in a Queue." *Laser & Photonics Reviews* (2024): 2400323.
- [3]. Ahmed, Hammad, et al. "Dynamic control of hybrid grafted perfect vector vortex beams." *Nature Communications* 14.1 (2023): 3915.

Single-Stage Fiber Amplifiers Achieving Linewidths at the Tens-of-kHz Scale for Quantum and Semiconductor Applications

Enkeleda Balliu, Peter Jänes, Gunnar Hedin, Gunnar Elgcróna, Håkan Karlsson

Cobolt AB – a part of HÜBNER Photonics, Vretenvägen 13, 17154, Solna Sweden

The use of an integrated high performance DPSS ring-cavity laser as a seed enables single-stage fiber amplification of the herein presented fiber laser system thereby opening the possibility for a smaller footprint and affordable cost structure compared with fiber laser solutions which need multi-stage amplification to achieve similar high average powers. In addition to achieving high average power, the single-stage amplification not only results in very narrow sub 100 kHz spectral linewidths but also ultra-low relative intensity noise (RIN) performance without active noise cancellation as well as very high optical signal to noise ratio.

The use of a thermo-mechanically stabilized seed combined with robust fiber amplification technology ensures reliable 24/7 operation. The beam delivery head is detachable from the delivery fiber, which facilitates integration of the laser system as an OEM component in instruments or other laser systems.

The narrow linewidth, ultra-low RIN (Figure 1), high-quality beam profile and detachable beam delivery head makes this single-stage fiber amplification laser system highly suitable for use in the creation and controlling of qubits based on neutral atoms as well as in ultra-sensitive particle analysis equipment used in semiconductor manufacturing fabs and for pumping of other laser systems.

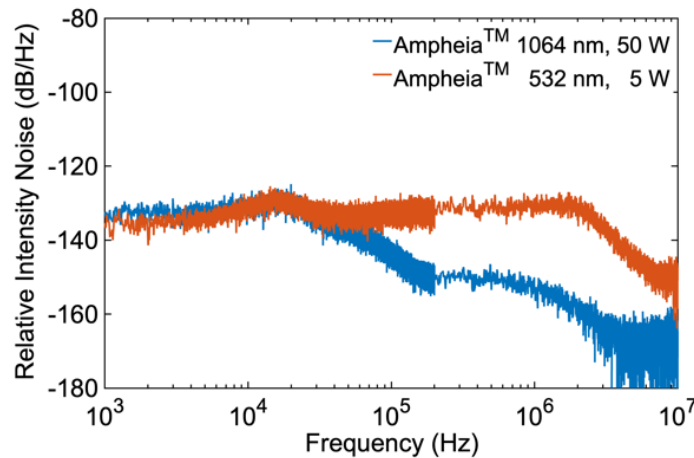


Figure 1: Relative intensity noise (RIN) of the unique single-stage fiber laser system, Ampheia™, at both 1064 nm and 532 nm.

An adaptive photonic nulling interferometer for the direct detection of exoplanets

P. Chingaïpe¹, D. Defrère¹, R. Laugier¹, L. Labadie²

1. Institute of Astronomy, KU Leuven, Celestijnenlaan 200D, 3001 Leuven, Belgium

2. I. Physikalisches Institut, Universität zu Köln, Zùlpicher Str. 77, 50937 Köln, Germany

Nulling interferometry is a promising method to directly image high-contrast exoplanets in a region of the parameter space that has so far only been covered by indirect detection methods. The high angular resolving power provided by mature infrastructure for long-baseline interferometry can aid this endeavour. These include the Very Large Telescope Interferometer (VLTI) and the Centre for High Angular Resolution Astronomy (CHARA), which routinely combine four and six telescopes, respectively. A nuller records the observed flux of a faint off-axis planet that is acquired by a finite number of nulled outputs after the light from an on-axis star has been optically redirected toward one or more bright outputs. While the traditional approach is to use bulk-optics based interferometers, the necessary routing, beam splitting, and recombination can be performed with photonic integrated circuits (PICs).

Although the use of interferometric nulling for the detection and characterisation of exoplanets is a tantalising prospect, it encounters many practical challenges when deployed on telescopes. The largest limitation being the extreme sensitivity of a nuller to amplitude and phase errors between the incoming telescope beams, which leads to a time varying stellar flux leakage in the nulled outputs. To prevent this systematic noise from becoming the dominant source of noise, fine wavelength dependent corrections to the amplitude and phase of the electric field can be applied with a PIC adaptive nuller exploiting the use of arrayed waveguide gratings, Mach-Zehnder interferometers and phase shifters. Here, I present a concept of a PIC adaptive nuller that builds on the heritage of the passive Asgard/NOTT PIC, which will be the first nulling interferometer on the VLTI.

Title:

Flow and Light: From Microboiling to Controlled Particle Transport Around Nanostructures

Authors:

Pantea Dara, Khosro Zangeneh Kamali, Steven Jones, Mikael Käll

Department of Physics, Chalmers University of Technology, 412 96 Göteborg, Sweden

Presented by: Pantea Dara, Postdoc

Abstract:

Controlling microscale fluid motion and temperature distribution using light offers powerful possibilities for on-chip manipulation, mixing, and pumping. In this work, we explore optically induced microflows and localized boiling phenomena generated by photothermal heating of nanostructures. First, we demonstrate how the design and optical absorption properties of metallic (gold) and dielectric (amorphous silicon) nanostructures can be tailored to direct fluid flow within microfluidic environments, enabling active transport of suspended nano-objects. Under continuous-wave (CW) laser illumination, these nanostructures efficiently vaporize water to form microbubbles that drive strong Marangoni flows, capable of rapidly transporting microparticles over large distances. Finally, we combine optical heating with Raman thermometry to probe local temperature fields during microboiling around silicon nanodisks and thin films. The intrinsic Raman-active phonons of silicon allow precise temperature mapping through frequency shifts, making silicon nanostructures both the heat source and temperature probe. Taken together, these results offer new insights into photothermally driven microflows and microboiling, contributing to the development of optofluidic systems with controlled heat and flow at the microscale.

Simulation of Narrow Far Field and Narrow Linewidth 980 nm Lasers with Surface Gratings

Ada Lona Dumitrescu

Master's Student, Department of Applied Physics, KTH Royal Institute of Technology, Stockholm, Sweden

E-mail: aldu@kth.se

1. Introduction

Distributed feedback (DFB) and distributed Bragg reflector (DBR) lasers with buried gratings require overgrowth, complicating the fabrication and putting defect-prone processed interfaces in regions subjected to current flow, high optical field intensity, and high temperature, affecting laser performance and reliability. By using laterally coupled ridge-waveguide (LC-RWG) and etched-through ridge-waveguide (ET-RWG) surface gratings, the overgrowth is avoided and the processed interfaces are kept away from current flow, high optical field intensities, and heat generated in the active region.

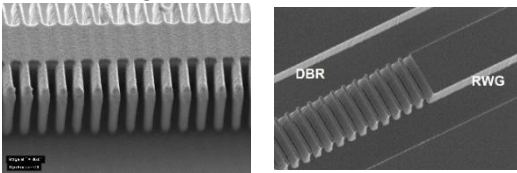


Fig. 1: Scanning electron microscopy pictures of LC-RWG (left panel) and ET-RWG (right panel) surface gratings (Courtesy of H. Virtanen, Tampere University)

2. Epilayer structure

The epilayer used a structured cladding to achieve a narrow vertical far field while maintaining a high quantum well optical confinement factor.

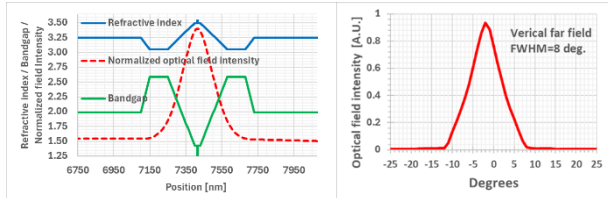


Fig. 2: 1D vertical distributions of the refractive index, bandgap and normalized optical field intensity around the single quantum well active region (left panel) and vertical far field with 8 degrees FWHM (right panel).

3. Transverse structures

The transverse structures have been developed for single transverse mode operation with low grating coupling coefficients to obtain narrow emission linewidths limited by a narrow reflectivity dip within the reflectivity stopband.

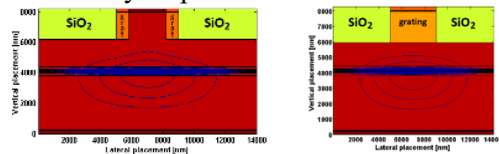


Fig. 3: Transverse profiles of the longitudinally averaged refractive index distributions and the corresponding optical field intensity distributions for the LC-RWG DFB (left panel) and for the ET-RWG DBR (right panel)

4 μm ridge width and 2.3 μm etching depth were chosen to ensure single transverse mode operation with high 2D QW optical confinement factor discrimination $(\Gamma_{\text{mode}_1} - \Gamma_{\text{mode}_n}) / \Gamma_{\text{mode}_1} > 0.5$, and vertical far field FWHM $< 13^\circ$. The LC-RWG is a 3rd order grating with 0.8 μm lateral penetration and 226/226 nm slice widths. The ET-RWG is a 5th order grating with 382/377 nm slice widths.

4. Longitudinal structures

The DFB laser has 14000 \cdot (226+226 nm) 3rd order LC-RWG grating periods, and a 452 nm phase shift at the middle, to a total length of ≈ 6.33 mm. The Master-Oscillator Power-Amplifier (MOPA) laser has a ≈ 38 μm long MO etalon RWG cavity bordered by 400 \cdot and 150 \cdot (377+382 nm) 5th order back and front ET-RWG DBRs, and ≈ 1 mm long PA after the front DBR, to a total length of ≈ 1.51 mm. The simulated lasers have AR coated facets.

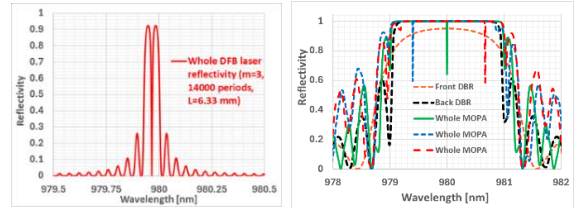


Fig. 4: Calculated reflectivity around 980 nm for the LC-RWG DFB laser (left panel) and for the DBR mirrors and the MOPA laser at 3 different MO bias (right panel)

The DFB laser stopband has $R > 0.92$, 0.07 nm FWHM, and a cavity dip of < 0.005 nm FWHM, while the MOPA laser stopband has $R > 0.999$, 2.23 nm FWHM, and a cavity dip of < 0.008 nm FWHM. Both lasers have vertical and lateral FWHM beam divergences of ≈ 12.5 and ≈ 4.5 deg., respectively, and reflectivity-limited emission linewidths.

5. Conclusions

The simulated DFB and MOPA lasers are suited for applications that require single transverse and longitudinal mode operation with narrow beam divergence and narrow emission linewidth. The DFB laser would provide a limited output power with a larger mode-hop-free tuning range, while the MOPA laser is much shorter and enables control and tuning of the emission wavelength through the MO bias, independently from the output power control through the PA. This enables mode-hop-free tuning only within the stopband and an independently controlled higher output power.

Characterization and testing of micro-force sensors designed for fibre integration in precision displacement detection

Jan Lukas Holleitner (M.Eng), Shiro Watanabe, Lee-Lun Lai, Kristinn B. Gylfason and Frank Niklaus
KTH Royal Institute of Technology, Department Micro- and Nanosystems

Force sensing is a key enabling technology for advanced research on microscale systems. Although a 3D printed tactile force sensor with optical read out is a promising approach, force sensors based on single cantilever designs have less design flexibility, resulting in less sensor sensitivity. Here we address this challenge by exploring the idea of mechanical amplification for fibre-printable micro-force sensors. The proposed structure, shown in figure 1, consists of a beam mounted on a semicircular spring (radius $40\ \mu\text{m}$) with dimensions of approximately $50 \times 100 \times 15\ \mu\text{m}$. In simulations the probe tip displacement is 1.4 times larger than that of the pin, producing signals that are $\sim 40\%$ stronger than the original, thereby possibly improving precision and signal distinguishability.

We demonstrated the displacement amplification by loading a force on the sensor pin observing its deformation in a SEM chamber. Figure 2 shows the loading test result, in which the behaviour of the force curve is nearly linear until $\sim 1.6\ \text{mN}$, with repeatability across multiple loading cycles (fig. 3). By analysing the SEM-images during the loading test, the displacement of the pin and probe tip was obtained as $10.3\ \mu\text{m}$ and $14.4\ \mu\text{m}$, respectively. As a result, the amplification mechanism successfully worked with the coefficient of ~ 1.4 . This holds potential in applications for biomedical diagnostics, material science, micromechanics and soft robotics.

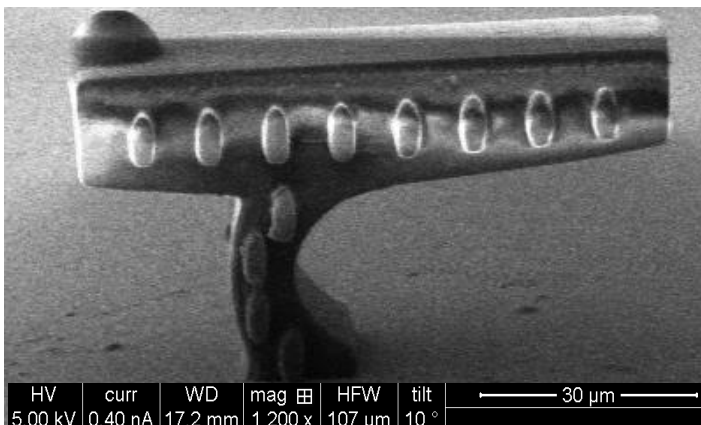


Figure 1: SEM image of the printed structure.

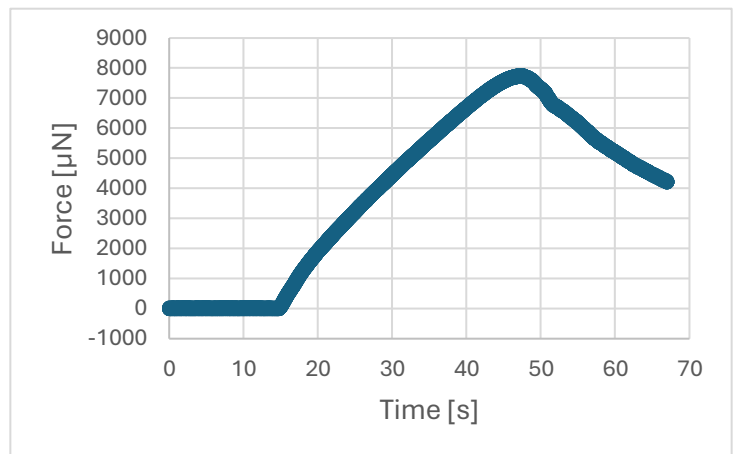


Figure 2: Force curve of a fracture test result. Increasing load was applied to the pin with a commercial force sensing probe at constant speed of $0.2\ \mu\text{m/s}$ until failure.

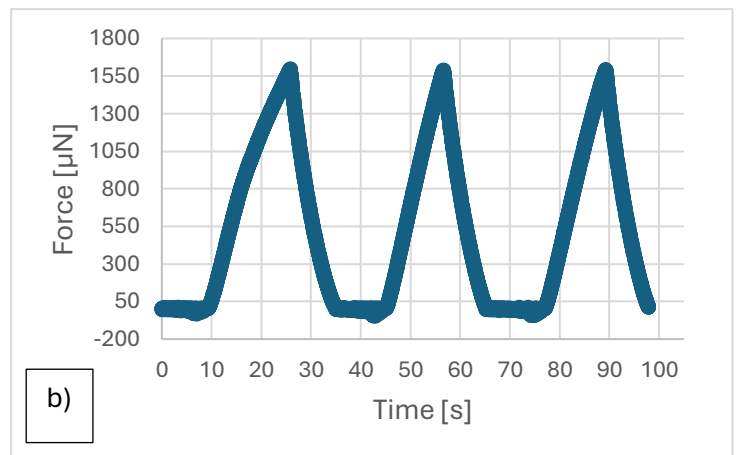
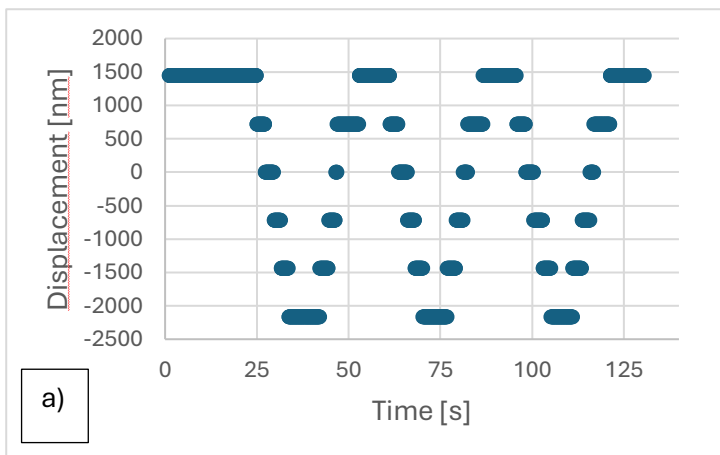


Figure 3: Displacement curve (a) and force curve (b) of a repetition test result. A load of $1.6\ \text{mN}$ was applied to the pin with a constant probe speed of $0.05\ \mu\text{m/s}$.

Polarization-Dependent Anapole States in Elliptical Nanodisks for Nonlinear and Filtering Applications

M.E.Kjellberg*, H. Kylhammar, and S. Anand

Department of Applied Physics, School of Engineering Sciences, KTH Royal Institute of Technology, Albanova University Center, Roslagstullsbacken 21, 106 91 Stockholm, Sweden

*corresponding author: mikkokj@kth.se

Sub-wavelength all-dielectric nanostructures can confine light in the visible and infrared spectral regions through Mie resonances, enhancing light-matter interactions for optoelectronic and nonlinear optics applications [1]. Optical anapole states in Si nanodisks enable high optical field confinement and novel ways for manipulating light scattering [2,3]. Furthermore, by vertically stacking nanodisks, the degree of field confinement can be significantly enhanced, opening new avenues for advanced photonic device design [4].

Anapole states, characterized by suppressed far-field radiation and enhanced optical field confinement, are promising for nanophotonic applications. By utilizing the high refractive index contrast between Si ($n \approx 3.5$) and SiO₂ ($n \approx 1.45$), we design vertically stacked Si nanodisks that support anapole states without requiring complex fabrication steps. This approach simplifies production and enables strong light-matter interactions. Additionally, we show wavelength selective transmission/reflection by tailoring the dimensions and arrangement of nanodisks, enabling functions such as filters and structural coloration.

Elliptical nanodisk stacks introduce geometric anisotropy, enabling polarization-dependent anapole excitation at two distinct wavelengths [5]. When light is polarized along the major axis, the anapole mode occurs at a shorter wavelength, while polarization along the minor axis shifts it to a higher wavelength. This dual-wavelength behavior, controlled by the aspect ratio of the elliptical disks, provides a versatile platform for nonlinear processes, paving the way for advanced devices like tunable frequency converters and ultrafast optical switches.

Acknowledgements: The work is supported by the Swedish Research Council – Vetenskapsrådet, grant 2019-05321 and the Swedish Energy Agency – Energimyndigheten; grant 49227-1 and P2023-01371.

References

1. A. I. Kuznetsov, A. E. Miroshnichenko, M. L. Brongersma, Y. S. Kivshar, and B. Luk'yanchuk, "Optically resonant dielectric nanostructures," *Science* **354**, (2016).
2. A. E. Miroshnichenko, A. B. Evlyukhin, Y. F. Yu, R. M. Bakker, A. Chipouline, A. I. Kuznetsov, B. Luk'yanchuk, B. N. Chichkov, and Y. S. Kivshar, "Nonradiating anapole modes in dielectric nanoparticles," *Nat Commun* **6**, 8069 (2015).
3. Y. Yang and S. I. Bozhevolnyi, "Nonradiating anapole states in nanophotonics: from fundamentals to applications," *Nanotechnology* **30**, 204001 (2019).
4. F. Vennberg, A. P. Ravishankar, and S. Anand, "Manipulating light scattering and optical confinement in vertically stacked Mie resonators," *Nanophotonics* **11**, 4755–4764 (2022).
5. M. Kjellberg, F. Vennberg, A. P. Ravishankar, and S. Anand, "Polarization-Enabled Tuning of Anapole Resonances in Vertically Stacked Elliptical Silicon Nanodisks," *Advanced Photonics Research* **5** (11), 2400009 (2024).

Broadband Anti-Reflectance by Disordered Si Nanodisks for Thin-Film Solar Cells

H. Kylhammar*, S. Zayouna, A. Dumitrescu, M.E. Kjellberg, and S. Anand

Department of Applied Physics, School of Engineering Sciences, KTH Royal Institute of Technology,
Albanova University Center, Roslagstullsbacken 21, 106 91 Stockholm, Sweden

*Corresponding author: hannaky@kth.se

We design and fabricate spatially disordered Si nanodisks by colloidal lithography for broadband antireflection and light trapping. Absorption is optimized for thin-film solar cells through control of the geometrical features, dimensions, and density of the nanodisks.

The development of semiconductor based metasurfaces enables light management for a wide range of optoelectronic device applications¹. Dielectric nanostructure arrays provide significant improvement in antireflection and light trapping for thin-film solar cells^{2,3}. The Mie resonant nanodisks are designed to induce forward scattering, implying a strong dependence on the nanodisk dimension and shape for the desired antireflection and wavelength dependent light scattering. We employ colloidal lithography as a scalable and cost-effective nanofabrication technique. This bottom-up approach enables the formation of large-area, nearly hyper-uniform disordered nanoparticle arrays. A disordered arrangement minimizes the effects from spatial correlation^{4,5}. The interparticle spacing is controlled by the ionic strength of the nanoparticle suspension medium, and the nanodisk height profiles can be controlled by changing the conditions of the dry etch process. We investigate the antireflective properties of disks of varying height profiles, ranging from nearly cylindrical to tapered.

The measured reflectance of the fabricated arrays is compared with finite-difference time-domain (FDTD) simulations. The scattering profiles from single nanodisks and from arrays are simulated and optimized to generate forward scattering into the Si substrate for targeted wavelengths to increase the path length for absorption. Our results show both the geometrical size and shape of the nanodisks and their spatial arrangement are important for enhancing solar light absorption in thin film Si solar cells.

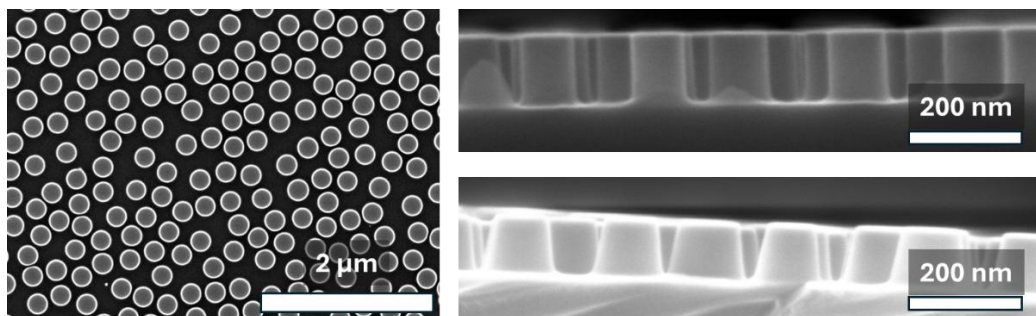


Figure 1. Left: Spatially disordered polystyrene nanoparticles (etch-masks) dispersed on Si substrate. Right: Si nanodisks fabricated by a pseudo-Bosch process; straight and tapered profiles.

Acknowledgements: The work is supported by the Swedish Energy Agency – Energimyndigheten, grant no. P2023-01371.

1. Son Tung Ha, Li Q., Yang, J.K.W., Demir H.V., Brongersma M.L., and Kuznetsov A.I. "Optoelectronic metadevices", *Science* 386(6725), eadm7442 (2024).
2. Kjellberg M., Ravishankar A.P., and Anand S. "Enhanced Absorption in InP Nanodisk Arrays on Ultra-Thin-Film Silicon for Solar Cell Applications," *Photonics*, 9, no. 3: 157, (2022).
3. Visser, D., Chen, D.Y., Désières, Y., Ravishankar A.P., and Anand S. "Embossed Mie resonator arrays composed of compacted TiO₂ nanoparticles for broadband anti-reflection in solar cells" *Sci Rep* 10, 12527 (2020).
4. Vennberg, F., Ravishankar A.P. and Anand S., "Manipulating light scattering and optical confinement in vertically stacked Mie resonators," *Nanophotonics*, Vol. 11, No. 21, 4755–4764, (2022).
5. Piechulla P.M., Fuhrmann B., Slivina E., Rockstuhl C., Wehrspohn R.B., Sprafke A.N. "Tailored Light Scattering through Hyperuniform Disorder in Self-Organized Arrays of High-Index Nanodisks," *Adv. Optical Mater.* 9, 2100186, (2021).

Femtosecond-laser-induced nanogratings for high frequency line filtering

Lee-Lun Lai¹, Shiqian Chen¹, Po-Han Huang², Göran Stemme¹, Frank Niklaus¹, Jiantong Li¹, and Kristinn B. Gylfason¹

¹KTH Royal Institute of Technology, Stockholm, Sweden

²National Tsing Hua University, Taiwan

The demand for miniaturized portable electronics has been growing in the recent decade and has driven the need for compact, high-performance on-chip power sources. Micro supercapacitors (MSCs) have emerged as promising candidates for on-chip filtering applications due to their high areal capacitance and planar architecture. However, most existing MSCs suffer from significant capacitance attenuation at high frequencies, limiting their effectiveness in modern electronic circuits operating above 10 kHz. This study addresses this challenge by developing a printed on-chip MSC with tunable electrode microstructure constructed by femtosecond-laser-induced nanogratings (Figure 1). The resulting 3D nanograting structure enhances capacitance while promoting rapid ion diffusion, crucial for maintaining high-frequency performance. The on-chip MSC demonstrates an areal capacitance of 1.2 mF cm^{-2} at 1 kHz and maintains 0.32 mF cm^{-2} at 10 kHz, outperforming previously reported on-chip MSCs, with a volume of only 0.0062 mm^3 (Figure 2). The integration of these nanograting structures offers significant potential for miniaturized, high-frequency line-filtering applications in advanced electronic systems, providing both high capacitance and excellent frequency response in a compact form factor.

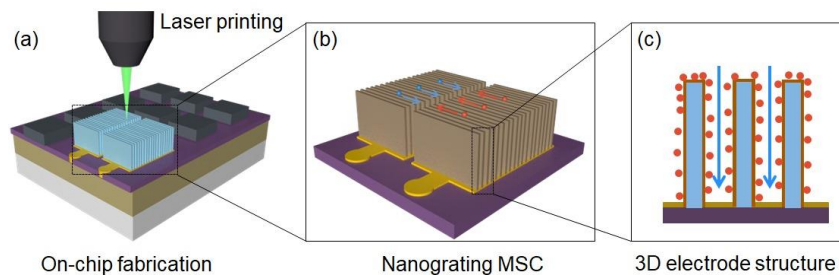


Figure 1: Fabrication process of the device.

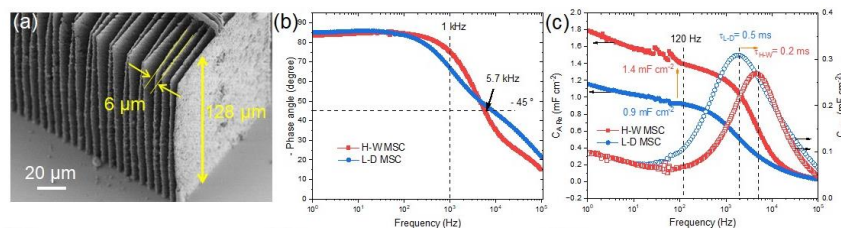


Figure 2: SEM image and electrochemical characterization.

PLASMON-ENHANCED GRAPHENE PHOTOTHERMOELECTRIC DETECTOR FOR MID-INFRARED SENSING APPLICATIONS

Pen-Sheng Lin¹, Shayan Parhizkar^{2,3}, Arne Quellmalz¹, Nour Negm^{2,3}, Stephan Suckow³, Aron Cummings⁴, Alba Centeno⁵, Amaia Zurutuza⁵, Max Lemme^{2,3}, Frank Niklaus¹, and Kristinn B. Gylfason¹

¹KTH Royal Institute of Technology, Sweden ²RWTH Aachen University, Germany ³AMO GmbH, Germany ⁴Catalan Institute of Nanoscience and Nanotechnology, Spain ⁵Graphenea S.A., Spain

Graphene is a promising detector material due to its broadband absorption and compatibility with Si photonics platforms [1]. However, coupling light to single-layer graphene remains a pivotal challenge. In this work, we address this challenge by integrating metallic plasmonic resonators with graphene to enhance the graphene-light interaction at 4.2 μm wavelength in the mid-infrared. This tripled the responsivity compared to a pure graphene device, attributed to enhanced graphene-light interaction. The low thermal mass of our miniaturized detector enables a fast frequency response of 25.6 kHz, enabling modulation to combat the $1/f$ noise typically dominating thermal detectors. The detector is bias-free, thus reducing noise and dark current. Our detector was implemented in a 150 mm silicon photonic (SOI) platform using standard optical lithography, showing its potential for on-chip integration and high-volume production. With these advantages, our detector is promising for emerging mid-infrared applications, such as mobile distributed carbon dioxide monitoring and medical diagnostics.

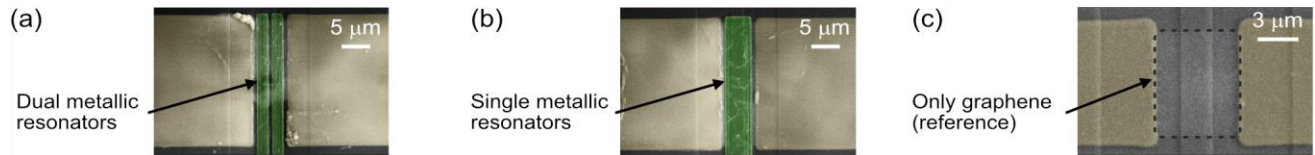


Figure 1: Device illustrations and their SEM images. (a) Dual and (b) single resonator types. (c) reference type.

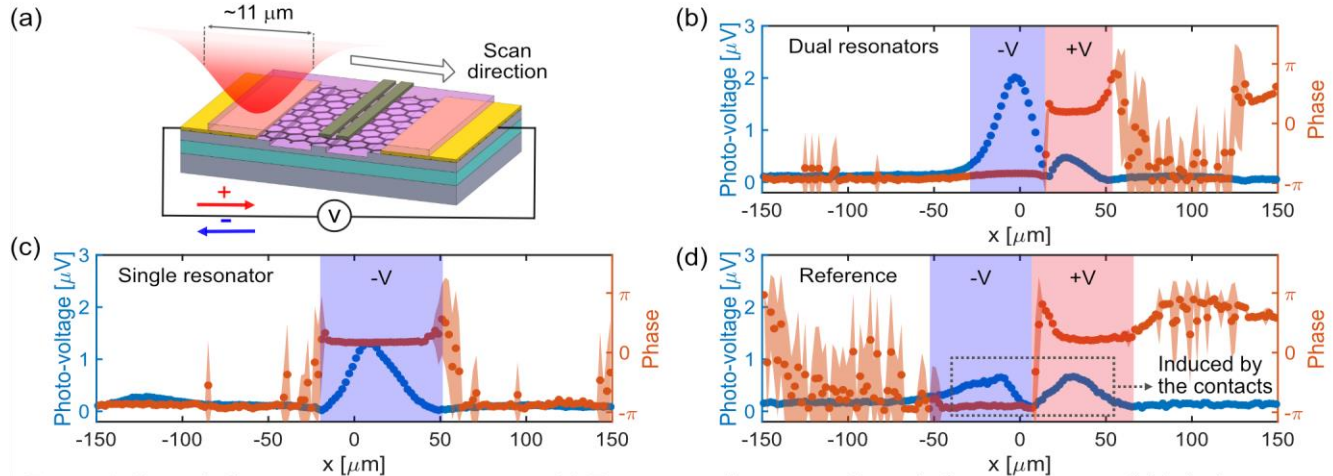


Figure 4: Spatial photo-response measurements, (a) Experiment illustration. Spatial photo-responses of (b) dual resonator type, (c) single resonator type, and (d) reference detector.

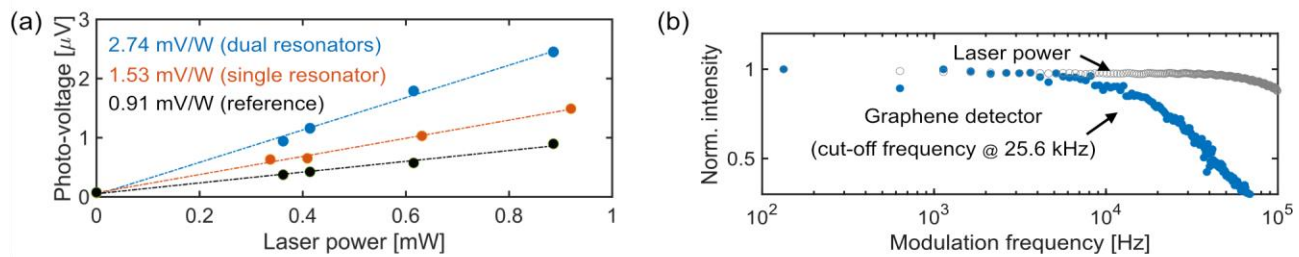


Figure 6: Characterization of the detector performance. (a) Responsivity. (b) Frequency response.

References

[1] F. H. L. Koppens, et al., Nature Nanotech. 9 (2014), pp. 780–793.

Towards InAs/GaSb Type-II Superlattice Growth by MOCVD, N. Mayner (a,b) ,
M. Delmas (a) , M. Hammar (b) , A. Strömberg (b), Y. Sun (b) , E. Costard (a) , and L.
Höglund (a)

(a) IRnova AB, Isafjordsgatan 22, 16440 Kista, Sweden

(b) KTH - Royal Institute of Technology, Department of Electrical Engineering 16440 Kista,
Sweden

Nanomotion Measurement in soil bacteria *Myxococcus xanthus*

This project aims to measure bacterial nanomotion with unprecedented spatial and temporal resolution. Traditional techniques such as atomic force microscopy, quartz crystal microbalance, surface plasmon resonance, impedance sensing, and graphene drum systems typically capture nanomotion at the whole-cell or population level. While powerful, these ensemble measurements often conflate biologically relevant signals with background mechanical noise, limiting their ability to resolve localized cellular dynamics.

Our approach introduces a localized, optically driven method that probes different regions of a bacterial surface using gold plasmonic nanorods. By employing a circularly polarized light beam, we can trap and rotate the nanorods at kilohertz frequencies, enabling the detection of minute changes in their rotational dynamics induced by bacterial motion. The nanorods are confined laterally in two dimensions by the optical trap's gradient force, while their vertical position is governed by a balance between the beam's scattering force and the Coulombic repulsion between the negatively charged bacterial surface and the gold nanorod. This configuration allows the nanorods to act as highly sensitive transducers of nanoscale mechanical fluctuations at specific surface locations.

In this work, we present the first nanomotion measurements performed on the soil bacterium *Myxococcus xanthus*. The selection of *M. xanthus* for our initial experiments helped mitigate several experimental challenges, such as surface adhesion control. At the same time, its distinctive social, developmental and gliding motility behaviors offer exciting opportunities to explore bacterial nanomotion within more complex, cooperative systems—extending the study beyond the extensively characterized model organisms *Escherichia coli* and *Bacillus subtilis*.

Thanks in advance,

Laura Pérez

Photonic Devices and Integrated Circuits for Sensing Applications

Gabriela A. Prando¹, Edvins Letko², Huiwen Li³, Olof Öberg¹, Simon Watanabe¹, Darius Jakonis, Anis Moradikouchi, Ingemar Petermann¹, Arthur Bundulis², Valdas Pasiskevicius³, and Qin Wang^{1*}

1 Research Institutes of Sweden (RISE), Sweden

2 Institute of Solid-State Physics (ISSP), Riga, Latvia

3 Division of Light and Matter Physics, Royal Institute of Technology (KTH), Sweden

Microfabricated photonic devices span a wide range of applications, including sensing, communication, and signal processing, enabling compact, high-speed, and low-power systems for chemical and environmental monitoring.

In this work, we present a SU-8 polymer waveguide-based Lossy-Mode Resonance (LMR) sensor for volatile organic compound (VOC) detection. The device was designed and fabricated with a focus on improving optical coupling to achieve high sensitivity, enhanced stability, and reduced optical losses. The use of SU-8 enables low-cost processing through mature lithographic microfabrication techniques, making this approach attractive for scalable production [1].

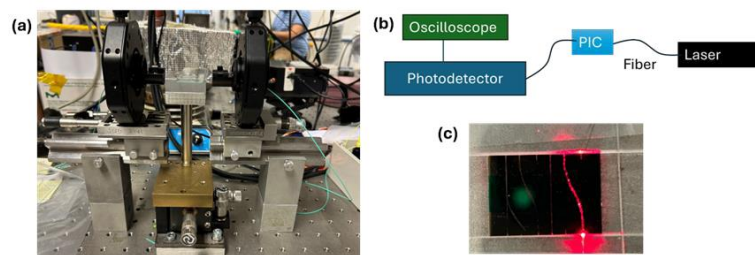


Figure 1(a) Experimental validation device setup, (b) Simplified schema and Illuminated SU8 waveguide

Additionally, we work with graphene/metasurface-based sensors, demonstrating the potential of integrating advanced materials with photonic architectures to high-performance sensing platforms—extending capabilities from infrared sensing [2] to the recent development of THz detectors.

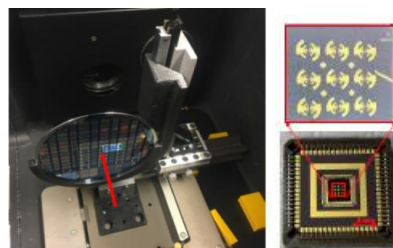


Figure 2 Wafer scale fabricated graphene/meta-surface integrated IR sensors (b) Wafer scale fabricated graphene/meta-surface integrated IR sensors

[1] E. Letko, A. Bundulis, and G. Mozolevskis, “Theoretical Development of Polymer-Based Integrated Lossy-Mode Resonance Sensor for Photonic Integrated Circuits,” *Photonics* 9 (10), 2022.

[2] Tom Yager, George Chikvaidze, Qin Wang and Ying Fu, Graphene Hybrid Meta-surfaces for Mid-Infrared Molecular Sensors, *Nanomaterials* 2023, 13, 2113. <https://doi.org/10.3390/nano13142113>

[Type here]

Integration of Optical Fiber Sensors into Asphalt Layers from Laboratory Validation to Field Deployment

Nazila Safari Yazd¹, Carola Sterner¹, Marie Zandi¹, Ingemar Petermann¹, Josef Persson², Daniel Bruvik², Jonas Gröndal³, and Patryk Witkiewicz³

1. Research Institutes of Sweden, Isafjordsgatan 22, 164 40 Kista, Sweden
2. Swedavia AB, Stockholm Arlanda Airport, 190 45 Stockholm-Arlanda
3. Skanska Sverige AB, VTC Nordost, Rydholmsvägen 3, 19491 Upplands Väsby

Structural Health Monitoring (SHM) of infrastructure, including buildings, tunnels, bridges, and roads, is essential for improving safety, durability, and maintenance efficiency. Conventional monitoring techniques are often destructive, discontinuous, or limited in spatial and temporal resolution [1]. Optical fiber sensors (OFSs), by contrast, offer unique advantages such as small size, immunity to electromagnetic interference, and the ability to provide distributed measurements along the pavement structure. Among the OFSs, Fiber Bragg grating (FBG) is one of the ideal candidates for SHM, due to its high sensitivity and high resolution [2].

We present our investigation into the feasibility of embedding OFS and FBGs directly within asphalt layers. The investigation is part of the FIMA project [3], which intends to develop a robust monitoring system capable of capturing pavement behavior under real traffic conditions on airport pavements. Laboratory tests at Skanska evaluated the durability of FBGs under asphalt compaction and high temperatures ($> 150^{\circ}\text{C}$), Fig. 1a. All FBGs survived the integration process without spectrum deformation or significant power loss. Peak wavelength shifts were observed during and after the process, mainly due to temperature effects from hot asphalt and compressive strain after curing, Fig. 1b. Following successful lab validation, OFSs were installed in the asphalt layers of a taxiway at Arlanda Airport (Phase II), demonstrating their potential for reliable, real-time, and long-term pavement monitoring Fig. 1c.

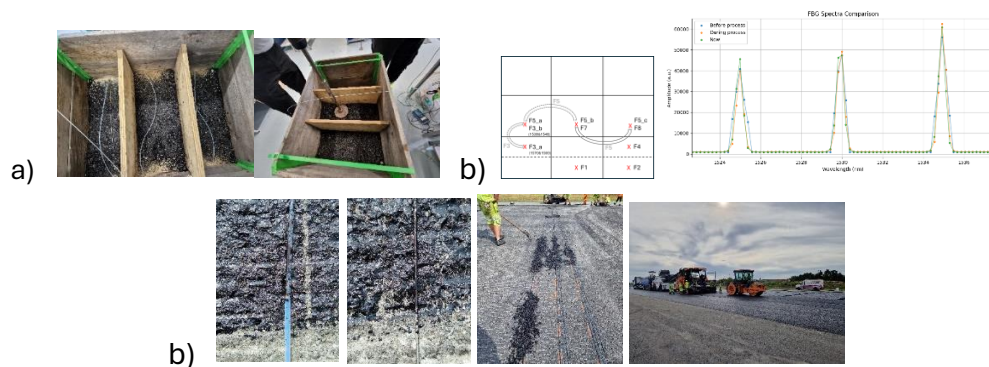


Fig. 1. a) OFS integration in simulated asphalt process at Skanska lab, b) asphalt bloc-OFSs layout, and c) integration of OFSs in a taxiway asphalt layers in Arlanda Airport.

References

- [1] M. F. Bado, *et al.*, "A Review of Recent Distributed Optical Fiber Sensors Applications for Civil Engineering Structural Health Monitoring"
- [2] M.H. Yassin, *et al.*, "Fiber Bragg gratings (FBG)-based sensors:a review of technology and recent applications in structural health monitoring (SHM) of civil engineering structures"
- [3] FIMA Vinnova-funded project; "<https://www.ri.se/en/expertise-areas/projects/advancing-pavement-monitoring-for-sustainable-airport-infrastructure>"

InP/Si Hybrid Photonic Crystal Surface-Emitting Lasers (PCSELS)

O. Sjödin, A. Charalampous, J. Jieensi, A. Strömberg and M. Hammar

KTH - Royal Institute of Technology, Department of Electrical Engineering 16440 Kista,
Sweden

Poster Abstract to OPS conference in Kista 2025

Titel: Combined lance system for real-time chemical analysis and temperature detection of steel melts

Authors: C. Sterner¹⁾, F. Sandberg²⁾, C. Nilsson³⁾, C. Mitra⁴⁾, J. Petersson⁵⁾, M. Spellas²⁾, T. Hellebjörk²⁾, F. Vighagen⁴⁾, C. Gardebring⁴⁾, D. Malmström⁵⁾, S. Bergqvist⁵⁾, M. Gilbert Gatty⁵⁾, and I. Petermann¹⁾

¹⁾RISE Fiberoptics and Photonics Unit, ²⁾Alleima Tube AB, ³⁾SSAB, Luleå, ⁴⁾Agellis Group AB, and ⁵⁾Swerim.

The Swedish steel industry produces small batches of advanced specialty alloys tailored to specific needs. A major challenge in process control is obtaining real-time data from key parameters directly from the molten steel. Currently, this monitoring is mostly manual, slow, and difficult to integrate into online systems.

In the RealSteel project we are developing a lance-based system to measure temperature and chemical composition in real time directly from the molten steel during production. This enables a more efficient process, reducing energy consumption and production costs. In the long run, it strengthens the competitiveness of Swedish steel producers and lowers the climate footprint of steel production, contributing to the green transition.

The lance concept builds on results from previous projects and focuses on two key processes in the steel plant; the ladle furnace, where both temperature and chemical composition are critical, and the tundish, where real-time temperature measurement will improve control of the casting process.

The lance system uses a ceramic lance to collect the radiation from within the melt for analysis. The temperature is measured with a Broadband Spectral Thermometer (BST) technology that estimates the temperature by analyzing the blackbody radiation spectrum from the melt. The chemical analysis is based on a Laser-Induced breakdown Spectroscopy (LIBS) technology, where the characteristic radiation obtained from a laser-generated plasma in the melt is analyzed.

The combined lance system is evaluated at one end-user's steel mill. Previous project's results give that temperature trends can be followed that is a valuable tool for the steel mill operators. Further, the chemical analysis is improved to meet the steel producers' demands for alloy content.

The lance system is a promising tool for the steel producers to obtain an improved production process that will consume less energy and hence a lower production cost. In the long term, this strengthens the competitiveness of Swedish steel producers while reducing the climate footprint of steel production.

The project has been carried out within the Strategic Innovation Programme Process Industrial IT and Automation, a joint venture by Vinnova, Formas and Energimyndigheten.

Reference: M. Gilbert Gatty, C. Sterner *et al.*, Combined real-time temperature and chemical analysis of molten steels for production applications, Proceedings Nordic LIBS 2024 (32).

Abstract of a poster to OPS2025

Advanced Chip Technologies for Enabling Photonic and Quantum Innovations

Qin Wang

Smart Hardware Department, Research Institutes of Sweden, RISE AB

Semiconductor chips are the important bit of hardware for many applications in our daily life such as smartphones, innovative medical devices, and core components in electric vehicles. This poster presents a Vinnova competence center on Advanced Chip Technologies (ACT), which gathers semiconductor actors in Sweden to meet industrial/society needs by utilizing the scientific excellence and innovations. The ACT center has 17 partners including three academic partners Lund University, KTH and RISE and industrial partners ranging from start-ups to multinational companies with a wide and extensive network worldwide.

RISE has long term experience in design, fabrication and characterization of semiconductor-based devices and systems. It can be utilized as a technology platform to make valuable contribution for sustainable growth of Swedish industry in the related fields. A few types of photonic chips based on semiconductor quantum structures are presented here by exploring advantage of light to offer fast response, great bandwidth, especially their scalability for sensing, data center, telecom, and quantum applications.

Mechanical characterization of self-organized volume gratings produced by a femtosecond-laser-based 3D printing process

Shiro Watanabe¹, Lee-Lun Lai¹, Alexander Groetsch², Kristinn Gylfason¹, Frank Niklaus¹

1. Division of Micro and Nanosystems, School of Electrical Engineering and Computer Science, KTH Royal Institute of Technology
2. Division of Material and Structural Mechanics, School of Engineering Sciences, KTH Royal Institute of Technology

Abstract:

Micro 3D printing of structures made of glass materials is a promising fabrication method for the development of functional MEMS devices [1]. The advantages of rigidity, transparency, and chemical resistance of glass are beneficial for a wide range of applications. Our research group has previously presented the self-organized formation of glass gratings by irradiating hydrogen silsesquioxane (HSQ) with a femtosecond laser [2]. The 3D printing of glass gratings is interesting due to the fast-printing process and the capability to realize large structures with dimensions larger than 100 μm . However, during the production process, cracks and voids can occur, which influences the mechanical behavior of the printed structures. Thus, the purpose of this study, was to quantify how the grating influences the mechanical characteristics of the printed structures by means of uniaxial micro-compression testing.

Mechanical tests were performed using a micro-indenter (FT-I04, FemtoTools, Oxford Instruments) on a glass cube with a grating structure and an edge length of 30 μm , fabricated by femtosecond laser printing (Fig. 1(a)). After pre-test SEM imaging, the cube was compressed using a displacement-controlled cyclic loading protocol ($F_{\text{max}} = 10 \text{ mN}$) with complete unloading after each cycle ($N=5$). Load-displacement data were recorded during the test and converted to engineering stress and strain based on the cube geometry (Fig. 1b). The glass structure exhibited a nonlinear character and hysteresis between the loading and unloading process. It is assumed that voids and cracks inside the structure caused the mechanical response to be comparable to that of a foam structure. The elastic modulus was evaluated for each 0.05% strain interval along the stress–strain curve and plotted against to the square of the cube's height ratio h_i^2/h_t^2 , where h_i and h_t denote the cube's initial height and height during the loading. The elastic modulus shifts in proportion to the height ratio of the cube, following Ashby's open-cell model [3] (Fig. 1(c)). The result indicates that the mechanical response of the grating is close to a foam as its elastic modulus linearly shifted in the range of $h_i^2/h_t^2 > 1.02$, with a strain above 1.5 %. The behaviour with a small square height ratio is assumed to be buckling or fracture of sparse part or thin grating plate due to the nonuniform grating-plate size and a variation of density distribution in the cube. The maximum elastic modulus was 5.4% of that of solid 3D printed glass cubes reported in a previous study [1], which can be related to the grating structure's foam-like behaviour. In this study, we quantified the mechanical properties of a glass based grating structure elucidating its foam-like behaviour. Results will contribute to both device and process development of glass 3D printing techniques targeted towards applications in MEMS sensors and actuators for micro-manipulation.

Reference

- [1] P. H. Huang, et al., *Nature Communications* 14.1 (2023): 3305.
- [2] L. L. Lai, et al., *ACS nano* 18.16 (2024): 10788-10797.
- [3] M. F. Ashby, et al., "The mechanical properties of cellular solids." (1983): 1755-1769.

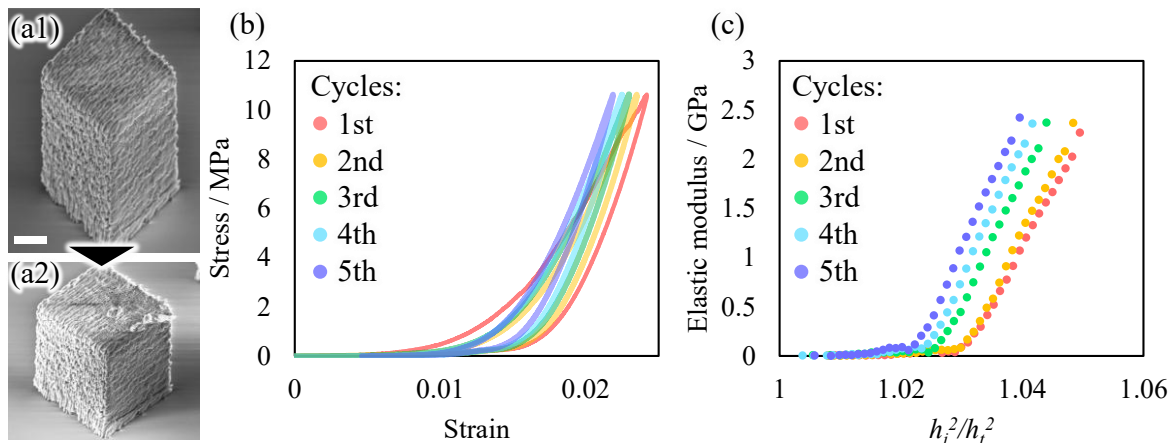


Fig. 1. Cyclic uniaxial micro-compression test. SEM images of a grating cube before and after loading are shown in (a1) and (a2), respectively, with a scale bar of 10 μm . The results of the loading test are illustrated by the stress–strain curves in (b) and the evaluated elastic modulus in (c).